New Characteristics of Zonal Flows in Multi-scale Plasma Turbulence

Jiquan Li 1,2), K. Uzawa 3), Y. Kishimoto 1), Y. Kouduki 1), Z. X. Wang 1)

1) Graduate School of Energy Science, Kyoto University, Uji, Kyoto 611-0011, Japan
2) Institute for Fusion Theory and Simulation, Zhejiang University, Hangzhou, China
3) National Institute for Fusion Science, Toki 509-5292, Japan

E-mail contact of main author: lijq@energy.kyoto-u.ac.jp

Abstract: The evolution of multi-scale plasma turbulence including resistive MHD and micro-instability is studied based on a 5-field gyrofluid simulation aiming to understand complex nonlinear interaction and turbulent transport. Here we report two new findings on the zonal flow (ZF) characteristics: (1) *A robust oscillatory ZF with finite frequency* is created in slab geometry for the first time due to the multi-scale interaction so that the ion heat transport is not efficiently suppressed. It is identified that the finite frequency ZF results from a magnetic island seesaw pivoted around the singular layer due to a net oscillatory electromagnetic torque, which is sustained by micro-instability through multi-scale interaction. These results imply probable relaxation of locking mode and degeneration of the favorable role of ITG ZFs in transport suppression in tokamak plasmas. (2) On the other hand, *a global ZF eigenmode* is found in Hasegawa-Mima(HM) model due to the radial spectral effect of ZFs, in which all components have the same enhanced growth rate. It is found that the global ZF eigenmode originates from successive cross coupling between ZFs and turbulent sidebands.

1 Introduction

The physics of multi-scale turbulence due to various linear and nonlinear instabilities with wider scale in magnetic fusion plasmas has attracted much attention recently [1-8]. Typically, like in tokamak plasma, the fluctuation is categorized as macro-scale MHD, ion and electron scale micro-turbulence as well as some anisotropic large scale structures such as the zonal flow (ZF). Turbulent transport is one of major concerns since it can lead to loss of plasma confinement performance in fusion devices. The multi-scale turbulence interaction may provide new destabilizing/stabilizing mechanism or anomalous free energy source/sink. Different scale fluctuations can directly interplay each other or indirectly affect through a ZF, which has been widely recognized as a stationary coherent structure [9]. The spatio-temporal nature of the ZF is of rather importance in plasma transport. Generally, the ZF can efficiently suppress plasma turbulence and reduce turbulent transport due to the property of low/zero frequency. However, it is geometrically coupled with a geodesic acoustic mode (GAM) in a toroidal plasma so that it behaves oscillatory [10]. This time-dependent property weakens its favorable suppression role in transport [11]. On the other hand, the spatial structure or

spectrum of the ZF is closely related to the shearing rate, which is a key index to evaluate its role in transport suppression. The ZF spectrum not only governs the suppression efficiency [12], but also may influence its nonlinear generation through a modulation instability in turbulence[13]. Hence, in this work, we focus on investigating the spatio-temporal characteristics of the ZFs with an emphasis of underlying physics mechanism of multi-scale nonlinear interaction.

In fusion plasma, the MHD fluctuation as a macro-scale structure is a significant ingredient, which may cause plasma disruption due to the dynamics of magnetic island. A typical example is the rotation and locking of the magnetic island [14,15]. It is intended to properly utilize it to control turbulent transport while a major disruption is avoided [16]. The dual effects of the nonlinear interplay between the MHD and micro-turbulence should be consistently considered in an integrated system. Meanwhile, the ZF, likely excited by MHD fluctuations, may hopefully play an essential role in the formation of transport barrier [17]. Here we perform a multi-scale turbulence simulation to investigate these issues.

2 Modeling equations for mixed resistive MHD and micro-turbulence

Aiming to understand underlying physics of multi-scale nonlinear interaction, a slab version of 5-field gyrofluid model is employed to perform multi-scale simulation [18]. Here the resistive (kink-) tearing mode (RKTM) and the ion temperature gradient (ITG) driven instability are sampled to represent the MHD fluctuation and the micro-turbulence, respectively. In a normalized form for the ion-scale drift wave, the model describing the mixed turbulence consists of the nonlinear evolution equations of continuity (density n), electrostatic potential ϕ (vorticity $\nabla_\perp^2\phi$), parallel component of vector potential $A_{//}$ (usually denoted by magnetic flux $\psi = -A_{//}$), parallel ion velocity $\upsilon_{//}$, and ion temperature T_i, as follows

$$d_t n = -\partial_y\phi - \nabla_{//}\upsilon_{//} + \nabla_{//} j_{//} + D_n\nabla_\perp^2 n \quad , \tag{1}$$

$$d_t\nabla_\perp^2\phi = (1+\eta_i)\partial_y\nabla_\perp^2\phi + \nabla_{//} j_{//} + \mu_\perp\nabla_\perp^4\phi \quad , \tag{2}$$

$$\beta\partial_t A_{//} = -\nabla_{//}(\phi - n) - \beta\partial_y A_{//} - \eta j_{//} + \sqrt{\tfrac{\pi m_e}{2m_i}}\left|\nabla_{//}\right|(\upsilon_{//} - j_{//}) \quad , \tag{3}$$

$$d_t\upsilon_{//} = -2\nabla_{//} n - \nabla_{//} T_i + \beta(2+\eta_i)\partial_y A_{//} + \eta_\perp\nabla_\perp^2\upsilon_{//} \quad , \tag{4}$$

$$d_t T_i = -\eta_i\partial_y\phi - \tfrac{2}{3}\nabla_{//}\upsilon_{//} - \tfrac{2}{3}\sqrt{\tfrac{8}{\pi}}\left|\nabla_{//}\right| T_i + \chi_T\nabla_\perp^2 T_i \quad . \tag{5}$$

with $j_{//} = -\nabla_\perp^2 A_{//}$, $\beta = 8\pi n_0 T_{i0}/B^2$, $\eta_i = \ln n/\ln T_i$, $d_t = \partial_t + \hat{e}_z\times\nabla_\perp\phi\cdot\nabla_\perp$, $\nabla_\perp^2 = \partial_x^2 + \partial_y^2$ and $\nabla_{//} = \partial_z + \hat{e}_z\times\nabla(A_{//0} + A_{//})\cdot\nabla_\perp$ in slab geometry $\vec{B} = B_0\hat{e}_z - \beta\nabla A_{//0}(x)\times\hat{e}_z$ with const B_0 and model equilibrium $A_{//0} = (B_0\lambda^2\hat{s}/2\beta)\cosh^{-2}(x/\lambda)$ [19]. Here x is the distance deviated from the singular surface, $\hat{s}$ measures local magnetic shear and λ is the gradient

length of axial equilibrium current. The normalization is employed as follows [5, 18,20]

$$(x/\rho_i ; y/\rho_i ; z/L_n ; \upsilon_{ti} t/L_n) \to (x; y; z; t) \ ,$$

$$(L_n/\rho_i)(\tilde{n}/n_0 ; e\tilde{\phi}/T_{i0} ; \tilde{\upsilon}_{//}/\upsilon_{ti} ; 2e\upsilon_{ti}\tilde{A}_{//}/\beta c T_{i0} ; \tilde{T}_i/T_{i0}) \to (n; \phi; \upsilon_{//}; A_{//}; T_i) \ ,$$

with $\rho_i = \upsilon_{ti}/\omega_{ci}$, $\upsilon_{ti} = \sqrt{T_0/m_i}$, $\omega_{ci} = eB_0/m_i c$ and $L_n^{-1} = d\ln n_0/dx$. In deriving these equations, the gyrofluid closure for kinetic Landau damping physics and classical cross-field dissipations ($D_n, \mu_\perp, \eta_\perp, \chi_T,$) for short wave components are used [21].

Both ITG and RKTM instabilities can be driven through controlling the ITG parameter $\eta_i (= d\ln T_i/d\ln n)$ and the resistivity η and coexist in an integrated turbulence system. With an emphasis on the multi-scale interaction, we simulate the nonlinear evolution of coexisting unstable RKTM and ITG instability by adjusting two key parameters: resistivity η and η_i. The growth rates show that they almost determine individually the tearing instability in low wave number region and the usual ITG instability around $k_y \approx 0.6 \sim 0.8$ as shown in Fig.1. In MHD regime the magnetic island is formed and the reconnection takes place. Meanwhile the ITG micro-instability is excited around the singular layer.

3 Nonlinear simulation of mixed RKTM and ITG turbulence

Guided by linear stability analysis, nonlinear simulations are mainly performed for three cases with different relation of growth rates (a) $\gamma_{MHD} > \gamma_{ITG}$, (b) $\gamma_{MHD} \approx \gamma_{ITG}$, and (c) $\gamma_{MHD} < \gamma_{ITG}$ to explore the dual interaction of these two instabilities with sparse spectra. An initial value code is run with fixed boundary condition in which the radial domain $L_x = 100$ (or 50) is much larger than the singular layer. The domain in *y* direction is taken as $L_y = 20\pi$ so that the longest wave-number component $k_y = 0.1$ corresponds to the usual $m = 1$ tearing mode in a toroidal or cylindrical plasma. Reference parameter setting is fixed as $\beta = 0.01$, $\hat{s} = 0.2$, $\lambda = 25$, $D_n = \mu_\perp = \eta_\perp = \chi_T = 0.01$. The time evolution of mixed turbulence shows four phases: the weaker instability is nonlinearly accelerated by the stronger

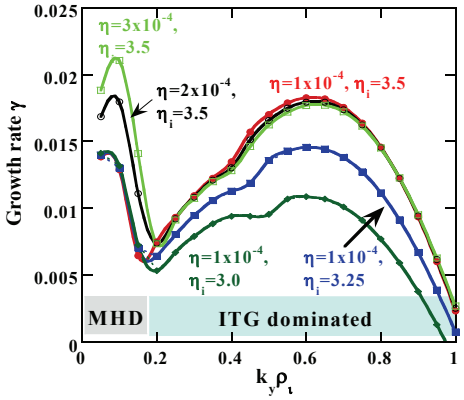

Fig.1 Linear growth rate of both RKTM and ITG modes for different resistivity η and ion temperature gradient η_i .

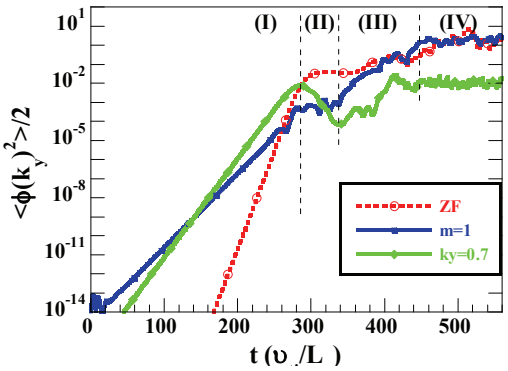

Fig.2 Time history of averaged kinetic energy $<\phi^2>/2$ for most unstable tearing (m=1) and ITG($k_y \approx 0.7$) components and the zonal flow. $\eta_i = 2$, $\eta = 2\times10^{-4}$

one (Phase I), in turn it leads to an initial saturation of the latter at lower level (Phase II). Afterwards, complex nonlinear interactions take place and the turbulent fluctuations increase again (Phase III) to saturate at a higher level in quasi-steady state (Phase IV), as illustrated in Fig.2 for the case (a). The energy flow between the MHD fluctuation and the ITG micro-turbulence can be explained through the spectral distributions of the mixed turbulence in Phases (II) and (IV) compared with ones of the classical MHD and pure electrostatic ITG turbulence as shown in Fig.3. The parametric dependence of the mixed turbulence spectra shows that the turbulence structure is determined by new magnetic reconnection geometry, but turbulence amplitude is sustained by the micro-instability through the multi-scale nonlinear interaction.

3.1 Magnetic island dynamics

Note that during the second increasing phase (Phase III), the initial equilibrium flux (or current) tends to be modified by the zonal field (or zonal current), the magnetic island is gradually formed. The zonal field nonlinearly modifies the initial equilibrium so that the RKTM and ITG modes tend to be destabilized, namely, the stability threshold is nonlinearly down-shifted. Finally a new equilibrium with magnetic island is achieved in Phase (IV). From Phase (III) to Phase (IV), the mixed turbulence develops into a dynamic system with an island seesaw pivoted around the singular surface, as visualized in Fig.4 by the snapshots of total flux (a-d) and much more clearly by the $m=1$ component (a'-d'). It is found that the magnetic fluctuation is dramatically enhanced in Phase (III) and the island seesaw occurs only

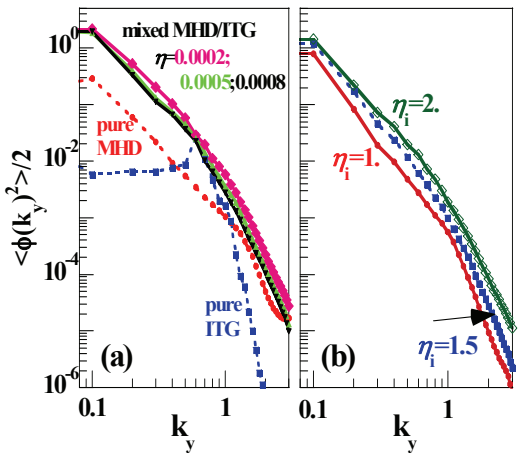

Fig.3 k_y spectra of mixed MHD tearing mode and ITG micro-turbulence in quasi-steady state for different η with $\eta_i = 2$ (a); and for different η_i with $\eta = 5\times10^{-4}$ (b). In (a) the spectra of pure ITG (square) and pure MHD (circle) are included for comparison.

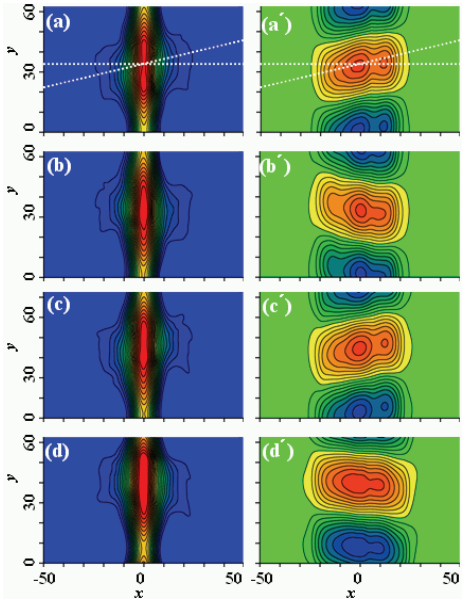

Fig.4 Snapshots of total magnetic flux (a-d) and the m=1 component (a'-d') corresponding to the maximum EM torque in (e). $\eta_i = 1.0$, $\eta = 5\times10^{-4}$.

when the ITG mode becomes unstable either linearly or nonlinearly. The kinetic free energy is pumped to the magnetic fluctuation through the nonlinear coupling. This process is manifested by the EM torque $T_{EMy}\hat{e}_z = \iint_{xy} x\hat{e}_x \times (\vec{j} \times \vec{B})_y dxdy$ exerting on the plasma produced by fluctuating EM force[22]. Fig.5 shows that the EM torque dramatically increases in Phase (III) and it is characterized by a time oscillation in Phases (III) and (IV). The maximum torque corresponds to the maximum amplitude of the island seesaw, showing a same frequency. The EM torque magnitude increases with the ITG instability as shown in Fig.6. Note that the ZF also behaves with a finite frequency as the island seesaw. The occurrence of the island seesaw is independent of the ZF but the latter can enhance the torque as the comparison in Fig.5. The oscillation frequency is about the diamagnetic drift frequency of the $m=1$ mode. It decreases as η_i becomes smaller than the linear stability threshold due to the zonal field, as shown in Fig.7(a). These evidences show that the ITG micro-instability provides kinetic free energy as a reservoir, the nonlinear interplay pumps it to the magnetic fluctuation to drive a net oscillating EM torque exerting on the plasma, then, the magnetic island experiences a seesaw oscillation based on the magnetic field frozen-in law in plasmas.

3.2 Zonal flow dynamics and heat transport

As an important nonlinear production, the ZF is a favorable component to regulate the turbulence and reduce the transport [9]. In slab geometry, it is characterized by a radially varying stationary, coherent structure. In tokamak, the ZF includes a finite frequency component due to the toroidal coupling with the geodesic acoustic mode (GAM) [10,18]. Its role in suppressing transport is therefore lowered. Here an oscillating ZF with a same frequency of the island seesaw is observed in the mixed turbulence in slab geometry for the first time, as shown in Fig.7(b). It is testified that the finite frequency is causally gained from the dynamic turbulence due to an oscillating component of the Reynolds and Maxwell stresses with the same frequency. The ZF level increases with the ITG instability. As one of

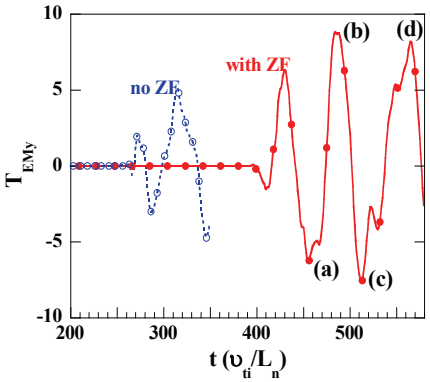

Fig.5 EM torque vs time corresponding to the island seesaw in Fig.4. $\eta_i = 1.$, $\eta = 5\times10^{-4}$

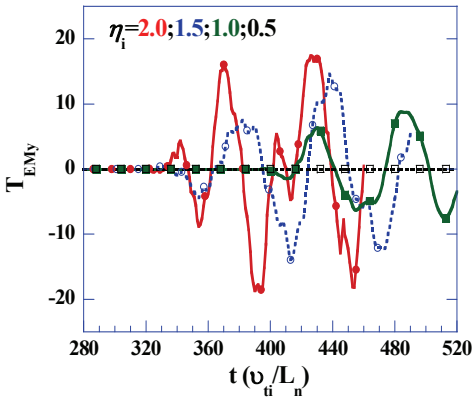

Fig.6 EM torque vs ITG instability. $\eta_i = 1.$, $\eta = 5\times10^{-4}$.

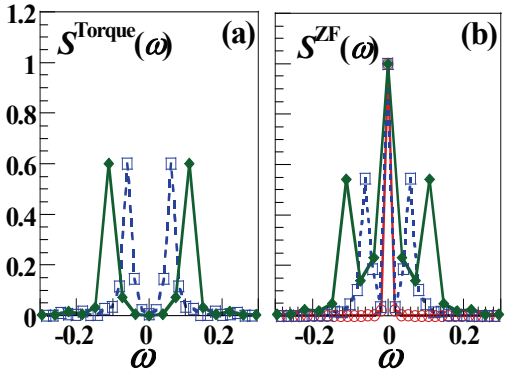

Fig.7 Frequency spectra of the ZF intensity $S^{ZF} \propto <\phi_{ZF}^2>/2$ *(a) and the EM torque intensity* $S^{ZF} \propto |T_{EMy}|^2$ *(b) for* $\eta_i = 0.5$ *(Circle); 0.75(Square); 1.5 (Diamond).*

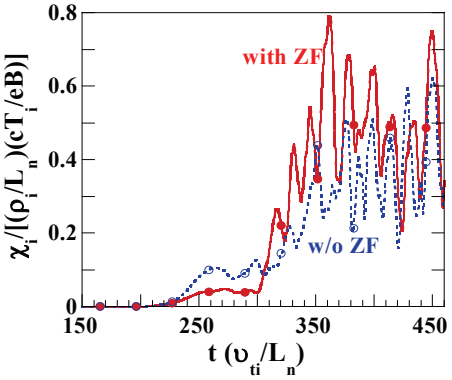

Fig.8 Turbulent ion heat transport $\chi_i \propto -<T_i \upsilon_x>$ *in the simulations with (solid) and without (dashed) zonal flow dynamics.* $\eta_i = 1.5$, $\eta = 5\times10^{-4}$.

main concerns, the turbulent ion heat transport is suppressed by the ZF only in Phase (II) before it becomes oscillatory. The transport level is still high even if the ZF is robust in Phase (IV) as shown in Fig.8. Comparisons show that the transport with the ZF dynamics is similar to, even slightly higher than that in the simulation without the ZF dynamics due to complex nonlinear interaction among micro-turbulence, MHD fluctuations and the ZF and also the zonal field. The result that the oscillatory ZF fails to reduce the transport can be understood as a natural result of the time-dependent ZF dynamics [11], a similar behavior of the GAM in tokamak plasmas [10,18].

4 Global zonal flow eigenmode

While the temporal characteristic of the ZFs is of importance in understanding its role in multi-scale turbulence, the spatial spectral effect of the ZF on its generation and the back-reaction to turbulence is another key issue. To address this problem, we assume that both the ZF and the pump have a radial structure or a spectrum with initial phase factors. In this case, the ZF components may couple together with all components of the pumps through nonlinear interaction based on the principal three-wave coupling so that the ZF generation may be modified. To inspect such physical process, we analyze the turbulence-ZF system by using the Hasegawa-Mima (HM) equation in a 2D (x, y) plane. A full spectral code is developed to solve the HM equation for given pump spectrum with different initial phase factors (representing the complex amplitudes). By choosing appropriate parameters, calculations show that for given pump spectrum, the ZF growth rate depends on the initial phase factors. All radial components of the ZFs have the same enhanced growth rate, as shown in Fig.9. This result indicates that the ZF components couple each other, exhibiting global nature as an eigenmode. We refer to it as a *global ZF eigenmode*. It is qualitatively different from the common understanding that the ZF components can be regarded to be independent so that a monochromatic zonal mode could be sampled to describe the generation

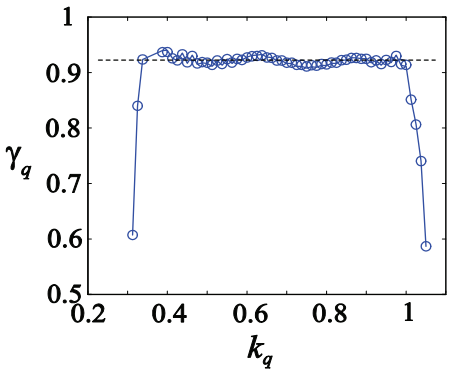

Fig.9 Growth rates of the ZF as a function of the radial wave number of ZF. It shows that all components couple each other with same growth rate.

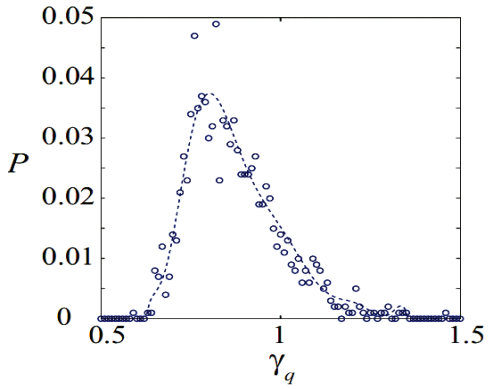

Fig.10 Probability density function(PDF) with respect to the growth rate of coupled ZF eigenmode for given pump spectrum and different initial phase factors.

process in modulation analysis. This new global ZF eigenmode seems to be similar to the global toroidal drift wave in tokamak plasmas in form. It is identified to originate from a successive cross coupling with the corresponding sideband spectrum of the pumps, which can not only establish a global eigenmode, but also enhance the growth rate. Interestingly, it is found that the ZF growth rate is probabilistically determined by the statistical distribution of the initial phase factors of the pump mode, which may correspond to the turbulent fluctuation. This characteristic is statistically represented by the probability density function (PDF) with respect to the growth rate, i.e., $P(\gamma_q)$, for 1000 simulations under different pump structures generated by different sets of random initial phase, as shown in Fig.10. It exhibits a Gaussian like shape with a weak tail component in the high γ_q region. A minimal modeling with ten wave coupling has been proposed to understand the new ZF characteristics.[13]

5 Summary and conclusion

In summary, we have investigated the nonlinear interaction of mixed-scale resistive MHD and ITG turbulence by performing 5-field gyrofluid simulation in slab geometry. Simulations show that the evolution of the mixed scale turbulence experiences four phases under complex nonlinear interaction and finally arrives to a dynamic quasi-steady state with magnetic island. The zonal field is created to modify the initial equilibrium and enhance the MHD and ITG instabilities. Meanwhile a finite frequency ZF is also generated robustly. It is found that the spectral distribution is characterized by the MHD turbulence but the turbulence amplitude is determined by the ITG driving force. An island seesaw oscillation has been observed for the first time, which is identified to originate from a net oscillatory electromagnetic torque due to the multi-scale nonlinear interaction. The micro-turbulence provides the kinetic free energy. As a result, the ZF causally gains a finite frequency so that the turbulent ion heat transport is not efficiently suppressed. These results imply that the island seesaw may provide a possible

relaxation mechanism of the locking mode in a cylindrical or toroidal plasma, which is usually followed by a major disruption. On the other hand, the oscillatory ZF in multi-scale turbulence loses the favorable suppression role in transport. It suggests a possible energy flow channel in a turbulence-ZF system. On the other hand, we have explored the spatial characteristics of ZF generation based on HM turbulence model. A global ZF eigenmode with enhanced growth rate is found due to the ZF spectral effect, which leads to a successive cross coupling between the pumps and ZFs through the sidebands. The result shows that the generation of the global ZF eigenmode is statistically determined by the turbulence structure with a given spectral distribution.

Acknowledgements

This work was partially supported by the Grant-in-Aid from JSPS (No. 19560828 and No. 18340186) and by NSFC Grant No.10575032.

References

1 S.-I. Itoh et al., Plasma Phys. Controlled Fusion 44, 1311, (2002)
2 Jiquan Li and Y. Kishimoto, Phys. Rev. Lett. **89**, 115002(2002)
3 C.J. McDevitt and P.H. Diamond, Phys. Plasmas **13**, 032302 (2006)
4 J Candy, *et al*., Plasma Phys. Controlled. Fusion **49**, 1209(2007)
5 A. Ishizawa and N. Nakajima, Nucl. Fusion **47**, 1540 (2007)
6 S Nishimura, *et al.*, J. Phys. Soc. Japan 77, 014501(2008)
7 T. Gorler and F. Jenko, Phys. Rev. Lett. **100**, 185002 (2008)
8 F. Militello, et al., Phys. Plasmas 15, 050701 (2008)
9 P. Diamond, et al., Plasma Phys. Control. Fusion 47 (2005) R35
10 K. Hallatschek and D. Biskamp, Phys. Rev. Lett. **86**, 1223 (2001)
11 T.S. Hahm and K.H. Burrell, Phys. Plasmas **6**, 922 (1999)
12 H. Biglari, P. H. Diamond, and P. W. Terry, Phys. Fluids B 2 (1990) 1
13 K. Uzawa, et al., Plasma and Fusion Research: Rapid Communications 3 (2008) 011
14 A.I. Smolyakov, *et al*., Phys. Plasmas **2**, 1581 (1995)
15 F. L. Waelbroeck and R. Fitzpatrick, Phys. Rev. Lett. **78**, 1703 (1997)
16 O. Gruber, et al., Phys. Rev. Lett. **83**, 1787 (1999)
17 D Grasso, et al., Plasma Phys. Control. Fusion 48 (2006) L87
18 N. Miyato, Y. Kishimoto and J. Li, Phys. Plasmas **11**, 5557 (2004)
19 N. F. Loureiro, *et al*., Phys. Rev. Lett. **95**, 235003 (2005)
20 J. Li and Y. Kishimoto, Phys. Plasmas **11**, 1493 (2004)
21 W. Horton, Phys. Rep. **192**, 1(1990)
22 R. Fitzpatrick, Nucl. Fusion **33**, 1049 (1993)